Published in JETP Letters 82, issue 1, 17-21, 2005
which should be used for any reference to this work

2D Laser Collimation of a Cold Cs Beam Induced by a Transverse *B* Field

M. D. Plimmer [1], N. Castagna [1], G. Di Domenico [1], P. Thomann [1], A. V. Taichenachev [2, 3], and V. I. Yudin [2, 3]

[1] *Observatoire Cantonal, 2000 Neuchâtel, Switzerland*
[2] *Novosibirsk State University, Novosibirsk, 630090 Russia*
[3] *Institute of Laser Physics, Siberian Division, Russian Academy of Sciences, Novosibirsk, 630090 Russia*
e-mail: Mark.Plimmer@ne.ch

We describe transverse collimation of a continuous cold cesium beam (longitudinal temperature 75 μK) induced by a two-dimensional, blue-detuned near-resonant optical lattice. The mechanism described for a lin-||-lin configuration is made possible by the application of a transverse magnetic field $B_\perp$. The phenomenon described differs from gray molasses, for which any small magnetic field degrades cooling, as well as from magnetically induced laser cooling in red-detuned optical molasses, where there are no dark states. The lowest transverse temperature is experimentally found to vary as $B_\perp^2$. The collimated flux density shows a dip as a function of $B_\perp$, the width of which is proportional to the cube root of the laser intensity, general features predicted by our semiclassical model. This technique provides a sensitive tool for canceling transverse magnetic fields *in situ* at the milligauss level.

PACS numbers: 32.60.+i

Continuous beams of cold atoms are useful for many physics experiments. Their flux density can be boosted by two-dimensional (2D) transverse laser collimation. Some schemes to achieve this with a 2D optical lattice (OL) use applied magnetic fields in addition to the lasers [1], while others should work better in zero field [2]. Both methods are designed to approach transverse temperatures close to the recoil limit (0.2 μK). The simplest approach is polarization gradient cooling (optical molasses (OM)) leading to temperatures of about 3 μK. With no polarization gradient, collimation can still be achieved if a transverse magnetic field ($B_\perp$) is applied. Conversely, one can use this technique to monitor transverse magnetic fields *in situ*. In this letter, we describe a study of laser collimation of a continuous cesium beam induced by a ($B_\perp$) for the $F = 3 \longrightarrow F' = 2$ component of the D_2 line and its implications for field cancellation.

For transitions of the type $J \longrightarrow J' = J$ or $J - 1$, cooling occurs for a laser tuned to the blue of the atomic resonance, while the presence of dark states in the ground hyperfine level leads to gray OM and, thereby, somewhat lower temperatures than those obtained with red-detuned OM ($J \longrightarrow J + 1$). In their study of the $F = 1$ to $F' = 1$ transition in ^{87}Rb in a 1D lin-θ-lin OM, Lucas *et al.* [3] measured temperature as a function of θ and concluded that the cooling observed near $\theta = 0$ arose from some residual polarization gradient. We have also investigated collimation as a function of θ in a 2D phase-stable power-recycling lattice [4]. To minimize θ, we adjusted the vertical input polarization of the input beam such that the extinction of the outgoing reflected beam, analyzed by a polarizing beam-splitter cube, was $<10^{-3}$. We still observed sub-Doppler temperatures but only when a transverse magnetic field was applied.

Although magnetically induced laser cooling (MILC) was described over a decade ago [5–8], most work has been on $J \longrightarrow J + 1$ transitions,[1] but published data on $J \longrightarrow J - 1$ transitions are rarer. Metcalf's group mentions results for the textbook case of 1D collimation of a ^{87}Rb beam on the $F = 1 \longrightarrow F = 0$ transition in a weak $B_\perp$ field with no polarization gradient (σ^+–σ^+ [9], lin-||-lin [10]). Nienhuis *et al.* [11] calculated a graph of reduced force versus reduced velocity for 1D cooling of a $J = 2 - J' = 1$ transition in a similar configuration but with a strong $B_\perp$ field and red detuning. The only work on Cs of which we are aware is by Valentin *et al.* [12–14], who studied the $F = 3 \longrightarrow F' = 2$ component of the D_2 line. There and in the experiments of Metcalf's group [5, 6], a thermal atomic beam was collimated in a 1D standing wave to sub-Doppler transverse temperatures in either strong magnetic fields

[1] Indeed, we observe the effect for red-detuned molasses using the $F = 4 \longrightarrow F' = 5$ component of the Cs D_2 line.

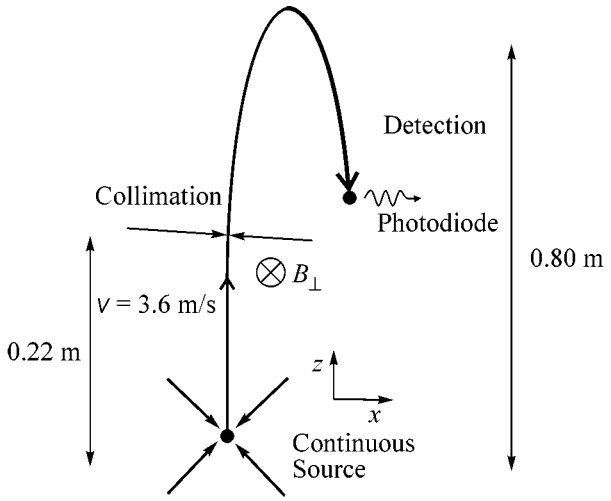

Fig. 1. Experimental setup for 2D collimation of a continuous Cs beam. The various lasers are tuned near hyperfine components of the D_2 line.

(Larmor frequency $\Omega_L \geq$ ground-state light shift Δ_{LS}) or weak ones ($\Omega_L < \Delta_{LS}$). In all of the above, the results describe cooling to zero transverse velocity $v_\perp$ in low fields and to $v_\perp \neq 0$ in high fields. All of the calculations were numerical simulations, and, to the best of our knowledge, no analytical expressions for the transverse temperature $T_\perp$ as a function of $B_\perp$ were given. Our own experiment is different in that it concerns 2D collimation of a continuous Cs beam using an OL with parallel linear polarization vectors; the magnetic fields are always weak ($B_\perp$ < 120 mG), and the atoms, already cold to begin with (longitudinal temperature 75 μK, $T_\perp$ = 60 μK), are transversely cooled to $T_\perp \approx 5$ μK.

In this letter, we present a detailed study of 2D MILC, including the influence of applied transverse magnetic fields on the atomic flux and final temperature for the case of an $F \longrightarrow F - 1$ transition. We show that, even if the mechanism appears on the blue side of the atomic resonance, it is different from usual gray molasses in two respects. First, gray molasses requires a polarization gradient, which is not the case here. Second, gray molasses is destroyed by a B field, be it transverse or longitudinal [15]. We outline the experimental arrangement and, then, present the results obtained, which show the striking contrast between the case of parallel polarizations (no polarization gradient, $\sin^2\theta < 10^{-3}$) and orthogonal ones (maximal gradient). Then, we compare our situation with gray molasses ($F \longrightarrow F$ or $F - 1$ with a polarization gradient). To gain some physical insight, we perform an extensive semiclassical analysis of MILC on $F \longrightarrow F - 1$ transitions in a linearly polarized standing wave. A qualitative picture of the Sisyphus cooling mechanism in the case under consideration is given. We find that, in a weak magnetic field, when the Zeeman splitting is less than the average light shift, the usually used slow-atom approximation fails due to a strongly nonlinear velocity dependence of the light force on the atom near $v = 0$. This can be qualitatively explained by high spatial gradients of the atomic density matrix and a small optical pumping rate near the field nodes. Instead, we obtain the nonlinear force dependence by numerical calculations, based on the expansion of the density matrix in a Fourier series that give results qualitatively similar to those found by experiment. Lastly, we present the transverse magnetic field cancellation procedure based on real-time measurement of the atomic flux.

The apparatus shown in Fig. 1 is akin to that of [1], where the z axis is vertical. Cs atoms from a moving OM are launched continuously in a parabolic flight with an initial velocity v_z = 3.6 m/s [16]. In a region above the source, the slow beam is collimated using a 2D linear-θ-linear OL with a $1/e^2$ intensity radius = 5.7 mm, truncated at a radius of 9 mm. We define I_1 as the average single-beam intensity in a circle of radius equal to the waist w. Here, a laser tuned 3γ above resonance with the $F = 3 - F' = 2D_2$ hyperfine component (where γ is the natural width of the excited state $6p\ ^2P_{3/2}$) is used in a phase-stable, power-recycling geometry with perpendicular, coplanar, counterpropagating beams [4]. These are reflected from gold-coated mirrors to maximize reflectivity (R > 97%) and minimize birefringence; improvement is expected from silver ones [17]. We observed that, when there is no polarization gradient, no collimation occurs unless one applies a transverse B field (but not a longitudinal one). A weak repumping laser (0.1 mW/cm^2) tuned to the $F = 4 \longrightarrow F' = 3$ hyperfine component of the D_2 line is added to improve cooling efficiency in the lattice. At the end of the flight, the atomic flux is probed via laser-induced fluorescence of the $F = 4 \longrightarrow F' = 5$ transition of the D_2 line. By adding a repumping beam in the probe region tuned to the $F = 3 \longrightarrow F' = 4$ transition, we can detect the atoms arriving in both the $F = 3$ and $F = 4$ hyperfine levels. We measure transverse temperatures by laterally translating the whole detection system (probe and repumping lasers and detection optics) in the horizontal plane and recording flux as a function of displacement. The data are fitted to a Gaussian curve (collimated atoms) superimposed on a slope representing the wings of a much broader distribution of uncollimated atoms. Depending on the atomic flux, resolutions of 0.2 μK can be achieved.

We have studied the variation of $T_\perp$ as a function of the mutual angle of inclination θ of the laser polarization vectors when $B_x = B_y = B_z = 0$. For θ = 0, the light field is a 2D lattice with an intensity gradient but uniform polarization and the temperature curve exhibits a local maximum. Still, for θ = 0, we have measured $T_\perp$ and flux versus $B_\perp$ (≤120 mG) when the other field components were cancelled out to within a few milligauss. For $B_x = B_z = 0$, the flux density curve (Fig. 2) shows a characteristic dip as a function of B_y. Similar

results are observed when $B_y = B_z = 0$, and we vary B_x. The width ΔB of the dip varies as the cube root of the lattice laser power over a range 1 to 32 mW (Fig. 3). The intensity of the weak repumping laser has no observable influence upon this width. The corresponding temperature curves exhibit a central maximum, coinciding with the value of $B_\perp$ that gives the smallest flux. Away from this maximum, we find that $T_\perp$ rises as $B_\perp^2$. This behavior is in striking contrast with the variation of flux density with B_z ($B_x = B_y = 0$), where we observe no collimation whatsoever. There is also a dramatic contrast with the behavior of flux versus $B_\perp$ for $\theta = 90°$, i.e., gray molasses, which displays a local central *maximum* at $B_\perp = 0$.

Cooling mechanism. Figure 4 shows the calculated adiabatic potentials, i.e., the eigenvalues of the total Hamiltonian of an atom at rest, including both the optical shift operator and the Zeeman shift operator. The four potential curves correspond to the dressed states, which, for $B_\perp = 0$, coincide with Zeeman substates of the ground $F = 3$ hyperfine level with the magnetic quantum numbers $m_F = \pm 2$ and $m_F = \pm 3$. They apply to the case of a weak $B_\perp$ and a linearly polarized standing wave ($\theta = 0$). The contribution due to off-resonant coupling with $^2P_{3/2}F' = 3$ is also taken into account. The energies are in kilohertz for the average lattice intensity of our experiment, namely, 3.5 mW/cm^2. Level crossing near the nodes is avoided due to the B-field mixing (the corresponding Zeeman splitting is taken as 5.3 kHz). In a weak magnetic field, the whole cooling process of transitions between the coupled $F = 3$, $m_F = \pm 2$ and noncoupled $F = 3$, $m_F = \pm 3$ dressed states takes place in the vicinity of the nodes, where the Zeeman splitting is comparable with the optical shifts. Outside these regions, all slow atoms are in the noncoupled states and so dissipate no kinetic energy. Let us consider an atom initially moving in the positive direction in one of the noncoupled states. Near the node (say, when $kx = 0$), it is likely to be coupled by the transverse B field to the dressed states with $m_F = \pm 2$, to climb uphill, and to dissipate its kinetic energy. Later (e.g., at $kx = 0.3$), when the dressed states $m_F = \pm 2$ become strongly coupled with light, it is optically pumped back to the noncoupled states $m_F = \pm 3$. Thus, the kinetic energy dissipated per cycle is of order of the Zeeman energy.

The Sisyphus mechanism [18] breaks down at a very weak magnetic field when an atom moving at the recoil velocity $\hbar k/M$ passes too quickly through the region of efficient B mixing for optical pumping to occur. This qualitatively explains the peak in temperature and the dip in the flux near $B_\perp = 0$. Let us estimate the Zeeman splitting at which it happens. The spatial size x of the region where the B mixing works is defined by $\Omega_R^2/(\delta(kx)^2) \approx \Omega_Z$ (the optical energy shift is comparable with the Zeeman splitting), where $\Omega_R \sin kx \simeq$

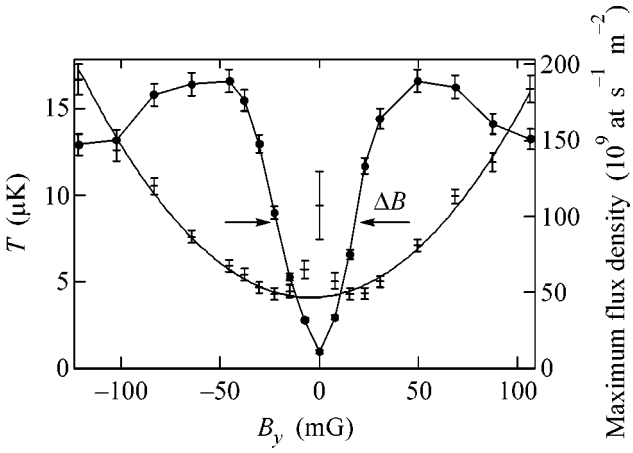

Fig. 2. 2D laser collimation using the Cs D_2 line in a lin-‖-lin lattice with $\theta = 0$, hyperfine component $F = 3 - F' = 2$, and detuning $+3\gamma$. Lattice laser power, 3.5 mW; repumping laser ($F = 4 - F' = 3$) power, 0.12 mW ($w = 5.7$ mm for both lasers). Variation of transverse temperature (+) and flux density (●) as a function of the transverse magnetic field B_y for $B_x = B_z = 0$. The polarization vectors of the lattice beams are along z, so there is no polarization gradient, and the other magnetic field components are cancelled. The solid line in the flux curve is to guide the eye; that in the temperature plot is a quadratic fit excluding the three central points.

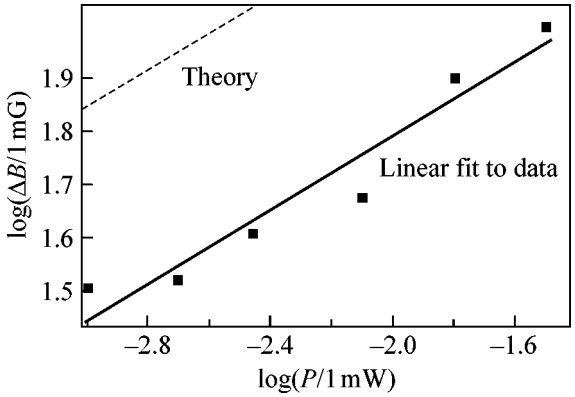

Fig. 3. Plot of the log of the width ΔB (mG) of Fig. 1 versus the log of lattice power P (mW) for $B_x = B_z = 0$. The slope of the linear fit (0.35(4)) suggests that $\Delta B \propto \sqrt[3]{P}$. The theoretical curve predicts the right slope and gives absolute values within a factor of two.

$\Omega_R kx$ is the local Rabi frequency in the vicinity of the well bottom averaged over the lattice volume and δ is the detuning. An atom with the recoil velocity crosses this region in a time $\tau = x(\hbar k/M)$. For efficient mixing in this time period, we need $\tau\Omega_Z \geq 1$, i.e., $\Omega_Z \geq [\omega_r^2\Omega_R^2/\delta]^{1/3}$, where ω_r is the recoil frequency. This power law is confirmed experimentally (Fig. 3) over a range of 30 in laser power. Note that, under our experi-

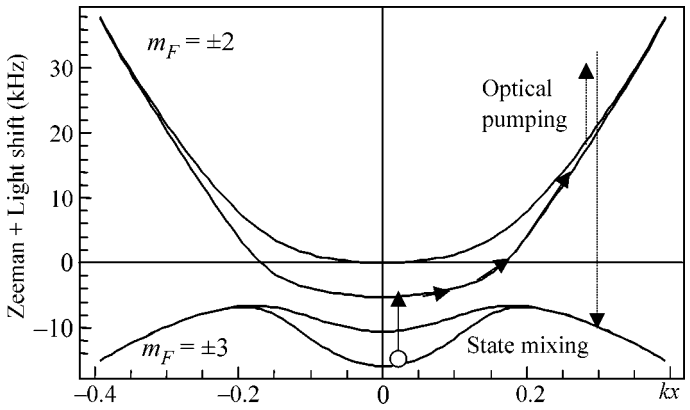

Fig. 4. Cooling principle in a weak magnetic field based on $F = 3 \longrightarrow F' = 2$ optical pumping between Zeeman sublevels of the $F = 3$ ground hyperfine level. Here, we show adiabatic potentials including both Zeeman and light shifts. The modulated light shift of the $m_F = \pm 3$ noncoupled levels arises from off-resonant coupling with the excited $F' = 3$, $m_{F'} = \pm 3$ levels. The value shown is for an average lattice laser intensity of 3.5 mW/cm^2.

mental conditions, the weak magnetic field regime always applies, since the Zeeman splitting is less than the average optical shift. However, in this limit, the condition for applicability of the usually used slow atom approximation is unusually stringent. Indeed, first, we require that

$$\frac{kv}{kx} \ll \gamma \frac{\Omega_R^2}{\delta^2}(kx)^2 \tag{1}$$

where γ is the spontaneous decay rate; i.e., the atom transit time through the region of efficient B-field mixing should significantly exceed the optical pumping time in the same region. In this region, the optical shift and Zeeman splitting are comparable:

$$\frac{\Omega_R^2}{\delta}(kx)^2 \simeq \Omega_Z \tag{2}$$

then

$$kx \simeq \sqrt{\frac{\Omega_Z \delta}{\Omega_R^2}} \ll 1. \tag{3}$$

Additionally, in order to neglect safely motional coupling between the dressed states, we also need

$$kv/kx \ll \mathscr{E} \simeq \Omega_Z, \tag{4}$$

where $\hbar\mathscr{E}$ is the energy separation between adiabatic potentials. Since the first condition is the more stringent, we have, finally,

$$kv \ll \Omega_Z \frac{\gamma}{\delta}\sqrt{\frac{\Omega_Z \delta}{\Omega_R^2}} \ll \Omega_Z. \tag{5}$$

If now we take $\delta = 3\gamma$, $\Omega_Z = 0.01\gamma$ (about 50 kHz), and $\Omega_R = \gamma$ (the corresponding intensity is about 8.8 mW/cm^2), we see that $kv < \gamma/100$; i.e., the corresponding velocity would be deeply subrecoil. Thus, in the weak magnetic field regime, there is hardly any room for the linear velocity approximation, estimates based upon which fail, and we need at least some kind of nonlinear theoretical estimates going beyond the slow-atom approximation. This led us to carry out a semiclassical numerical analysis of the problem.

Let us consider MILC in a linearly polarized monochromatic light field that excites a closed $F_g = F \longrightarrow F_e = F - 1$ transition. We approximate the actual field configuration by a 1D standing wave and neglect all other hyperfine levels. As the simplest model, we use a three-state system consisting of the noncoupled $|\mathrm{NC}\rangle$, coupled $|\mathrm{C}\rangle$, and excited $|\mathrm{E}\rangle$ states. Such a model reflects the main qualitative features of MILC on dark transitions. We take both the Doppler shift kv and Zeeman splitting Ω to be $\ll \gamma$ and assume that the laser field intensity and detuning correspond to the low-saturation limit:

$$S = \frac{1}{2}\frac{\Omega_R^2}{(\gamma/2)^2 + \delta^2} \ll 1. \tag{6}$$

There exist well-developed numerical methods to calculate the force and diffusion coefficient in an arbitrary 1D periodic light field. Typically, these are based on the expansion of the atomic density matrix in a Fourier series with subsequent numerical solution of a finite set of algebraic equations, obtained by the truncation of the original infinite set at some higher harmonic with number $n_{\max}$. An especially powerful tool for the force calculation is the continued fraction operator method, because, at each step, we need to invert a matrix of only low dimension whatever $n_{\max}$. The results for the spatially averaged force as a function of velocity are presented in Fig. 5. One can see a linear dependence very close to $v = 0$, a first Raman resonance at $kv \simeq \Omega_Z$ [6], and higher-order ones at $mkv \simeq \Omega_Z$ (with m an integer). The force behavior is qualitatively similar for the three-state model and for the $3 \longrightarrow 2$ transition studied experimentally.

One can evaluate the final momentum distribution $W(p)$ using the spatially averaged Fokker–Plank equa-

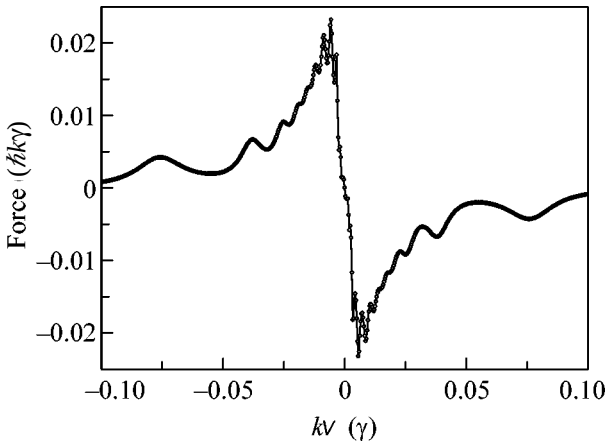

Fig. 5. Three-state model. The force in $\hbar k\gamma$ units versus kv/γ. The detuning $\delta = 3\gamma$, the Zeeman splitting $\Omega_Z = 0.01\gamma$, and the Rabi frequency $\Omega_R = \gamma$.

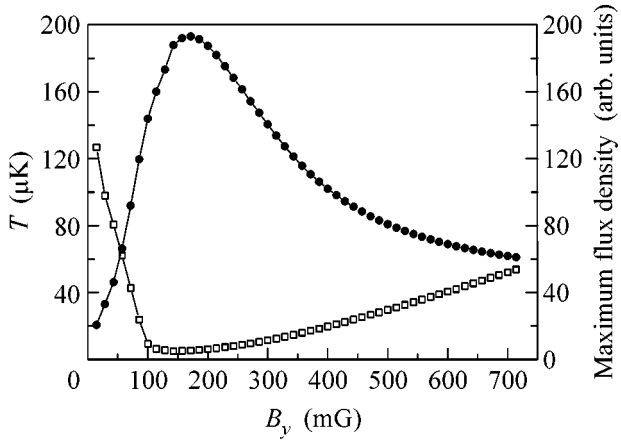

Fig. 6. Three-state model. Maximum flux density (●) in arbitrary units and the temperature (○) in microkelvin versus magnetic field in mG. The parameters are $\delta = 3\gamma$, $\Omega_R = \gamma$. There is qualitative agreement with experiment (Fig. 1, right-hand side).

tion. Typically, we observe non-Gaussian shapes and narrow double-peaked features near the zero momentum, which are gradually transformed into the peaks at nonzero velocities. To compare theory and experiment, we numerically calculate the Gaussian width w ($W(w) = W(0)/e$) and $W(0)$; the latter represents the maximal flux. We assume that $T \propto w^2$ and that $w = \hbar k$ corresponds to $T = 0.1$ μK. The results of such calculations, shown in Fig. 6, are qualitatively similar to experimental data. In particular, we see the "$B_\perp^2$" temperature dependence and a flux maximum offset slightly from the temperature minimum, as in Fig. 1. A detailed account of our theoretical models will be presented elsewhere.

Application: *in situ* compensation of $B_\perp$ fields. Three orthogonal pairs of Helmholtz coils provide the necessary static fields. The resolution of the current supplies leads to an uncertainty of ±2 mG for B_x and B_y and ±2.5 mG for B_z. Slow ambient fluctuations amount to ±0.2 mG for B_x and B_y and ±1.5 mG for B_z, and there subsist 50-Hz fields of <3 mG in all three directions. We start with 2D gray OM on the $F = 3 \longrightarrow F' = 2$ component of the D_2 line using a lin ⊥ lin configuration to provide the largest polarization gradient. Since any small magnetic field component leads to higher temperatures and lower flux, we adjust B_x, B_y, and B_z to *maximize* the flux. This first step is, thus, a bright-field technique. For a sensitivity <10 mG, we make the lattice polarization vectors parallel and vertical, so that B_x and B_y are the transverse fields. We then tune B_x and B_y to *minimize* the flux (dark-field method). To make B_z, the transverse field, the laser polarization should be horizontal. In 2D, this gives a polarization gradient and, thus, just gray molasses. However, by implementing a 1D lattice, one could also cancel B_z using MILC.

A.V.T. and V.I.Yu. are grateful to the Swiss National Science Foundation (FNRS) for financing an exchange visit. Their work is supported in part by the Russian Foundation for Basic Research (project nos. 05-02-17086 and 04-02-16488) and by INTAS (grant no. 01-0855). The authors thank D. Boiron and S. Pádua for supplying Ph. D. theses and C. Affolderbach and P. Berthoud for critical input. Experiments were partially supported by FNRS and METAS.

REFERENCES

1. G. Di Domenico *et al.*, Phys. Rev. A **69**, 063403 (2004).
2. A. V. Taichenachev *et al.*, Phys. Rev. A **63**, 033402 (2001).
3. D. M. Lucas, P. Horak, and G. Grynberg, Eur. Phys. J. D **7**, 261 (1999).
4. G. Di Domenico *et al.*, physics/0412072.
5. B. Sheehy *et al.*, Phys. Rev. Lett. **64**, 858 (1990).
6. P. van der Straten *et al.*, Phys. Rev. A **47**, 4160 (1993).
7. P. J. Ungar *et al.*, J. Opt. Soc. Am. B **6**, 2058 (1989).
8. D. S. Weiss *et al.*, J. Opt. Soc. Am. B **6**, 2072 (1989).
9. R. Gupta *et al.*, J. Opt. Soc. Am. B **11**, 537 (1994).
10. S. Pádua, PhD Thesis (SUNY, Stony Brook, 1993) (unpublished).
11. G. Nienhuis, P. van der Straten, and S.-Q. Shang, Phys. Rev. A **44**, 462 (1991).
12. C. Valentin *et al.*, Europhys. Lett. **19**, 133 (1992).
13. J. Yu *et al.*, IEEE Trans. Instrum. Meas. **42**, 109 (1993).
14. C. Valentin, PhD Thesis (Univ. de Paris-Sud, 1994) (unpublished).
15. C. Triché, P. Verkerk, and G. Grynberg, Eur. Phys. J. D **5**, 225 (1999).
16. P. Berthoud, E. Fretel, and P. Thomann, Phys. Rev. A **60**, R4241 (1999).
17. C. W. Goodwin, private communication (2004).
18. J. Dalibard and C. Cohen-Tannoudji, J. Opt. Soc. Am. B **6**, 2023 (1989).